Overview of the 12–14 March 1993 Superstorm

Paul J. Kocin,
Philip N. Schumacher,
Ronald F. Morales Jr.,
and Louis W. Uccellini
National Weather Service,
National Meteorological Center,
Camp Springs, Maryland

Abstract

An extratropical cyclone of unusual intensity and areal extent affected much of the Gulf and East Coasts of the United States on 12–14 March 1993. In this paper, the many effects of the storm will be highlighted, including perhaps the most widespread distribution of heavy snowfall of any recent East Coast storm, severe coastal flooding, and an outbreak of 11 confirmed tornadoes. A meteorological description of the storm is also presented, including a synoptic overview and a mesoscale analysis that focuses on the rapid development of the cyclone over the Gulf of Mexico. This is the first part of a three-paper series that also addresses the performance of the operational numerical models and assesses the forecasting decisions made at the National Meteorological Center and National Weather Service local forecast offices in the eastern United States.

1. Introduction

During the period 12–14 March 1993, one of the most intense extratropical cyclones in years, dubbed by some the "Storm of the Century," paralyzed much of the eastern United States. A combination of heavy snow, high winds, tornadoes, coastal flooding, record-low sea level pressures, and record-low temperatures affected the entire Atlantic seaboard, much of the Gulf Coast, portions of the Ohio Valley, Cuba, and parts of northern Mexico. The superstorm resulted in dozens of fatalities on land and at sea, hundreds of injuries, damage that was estimated to exceed $2 billion, and the most widespread disruption of air travel in the history of aviation.

Since this event affected nearly half the nation's population and was widely perceived by the media and the public as a forecasting "success," the storm provides an opportunity to 1) assess the progress made in forecasting midlatitude cyclones, 2) examine the performance of medium- and short-range operational numerical models in predicting a major cyclone event, 3) review the performance of forecasters who are challenged by the increasing amount of information available with numerical model products and with the often subtle differences that occur in the model guidance, and 4) illustrate the complex task of coordinating the issuance of watches and warnings that are required to save lives, reduce property loss, and alert the public of a large and dangerous weather event.

Three papers will describe various aspects of the storm. In this paper, a general meteorological description of the storm and a summary of its effects will be provided, including mesoscale surface analyses of the rapid development phase of the storm over the Gulf of Mexico. The synoptic overview and mesoscale discussion will describe the contributions of a variety of factors to the storm's development, heavy snowfall, coastal flooding, and severe thunderstorms and tornadoes. In the second paper of the series (Caplan 1995), the performance of the medium-range operational numerical models prior to the storm will be summarized and assessed. The models provided indications of a major storm for the eastern United States as early as four days prior to the initial development of the storm and six days before the peak of the storm with remarkable run-to-run consistency. In the third paper (Uccellini et al. 1995), an evaluation of the forecasting decisions within the Meteorological Operations Division (MOD) of the National Meteorological Center (NMC) and local forecast offices of the National Weather Service is provided, highlighting the successful forecast effort that culminated in the issuance of watches and warnings with lead times of one to two days.

2. Effects and impact of the storm

Reports in the press have mentioned that as many as 270 deaths may have been caused by the storm. However, fewer than 100 deaths can directly be attributed to the storm, according to the National Weather Service (NWS) disaster survey report (NWS 1994), with property damage estimated at approximately $2 billion. The economic loss that resulted from the

Corresponding author address: Paul J. Kocin, Meteorological Operations Division, NWS/NMC, 5200 Auth Rd., Camp Springs, MD 20746.
In final form 28 October 1994.

superstorm is greater than that associated with any recent extratropical storm. The storm curtailed business for tens of millions of people and produced the most widespread disruption of air travel in the history of aviation.

The superstorm produced a vast region of precipitation with amounts exceeding one inch (2.5 cm), extending from eastern Texas along the immediate Gulf Coast to nearly the entire East Coast. Maximum rainfall amounts were observed in Texas, where 6 in. (15 cm) fell.[1] The snowfall distribution from the Gulf Coast northeast to Maine is shown in Fig. 1. The areal distribution of significant snowfall is among the most widespread of any storm ever recorded in the eastern United States. The area enclosed by the 10-in. (25 cm) contour covers 170% to 300% of the equivalent area observed for any of the 23 snowstorms featured in Kocin and Uccellini (1990), exceeds 300% of the equivalent area for the March blizzard of 1888 (Kocin 1983), approximately 170% of the area of the widespread blizzard of 1899 (Kocin et al. 1988), and approaches the areal coverage of the 1831 snowstorm Ludlum (1968) describes as "the heaviest snowfall over the largest area of any storms in our period of study." Snowfall accumulations exceeding 40 in. (100 cm) are only rarely measured along the East Coast but were observed in at least seven states (Maryland, New York, North Carolina, Pennsylvania, Tennessee, Vermont, and West Virginia) with maximum amounts of 50 in. (125 cm) at Mount Mitchell, North Carolina, and 60 in. (150 cm) at Mount Leconte, Tennessee. The 13.0 in. (33 cm) at Birmingham, Alabama, was the greatest recorded for any day, month, or season at that site. Other record-breaking snowfall amounts include Chattanooga, Tennessee (20.0 in.; 51 cm), Beckley, West Virginia (30.9 in.; 78 cm), and Syracuse, New York (42.9 in.; 109 cm). While the axis of heaviest snows fell west of the Atlantic coast, all the major cities of the Northeast measured 10 to 12 in. (25 to 30 cm), on average, despite a changeover to ice pellets and rain. The combination of heavy snow, significant amounts of ice pellets, rain, and a sudden freeze had a major impact in the major cities since the underlying snowpack was exceedingly difficult to clear from streets and walkways. It is estimated that snowfall (greater than an inch; 2.5 cm) impacted the lives of 90 million people in the United States alone.

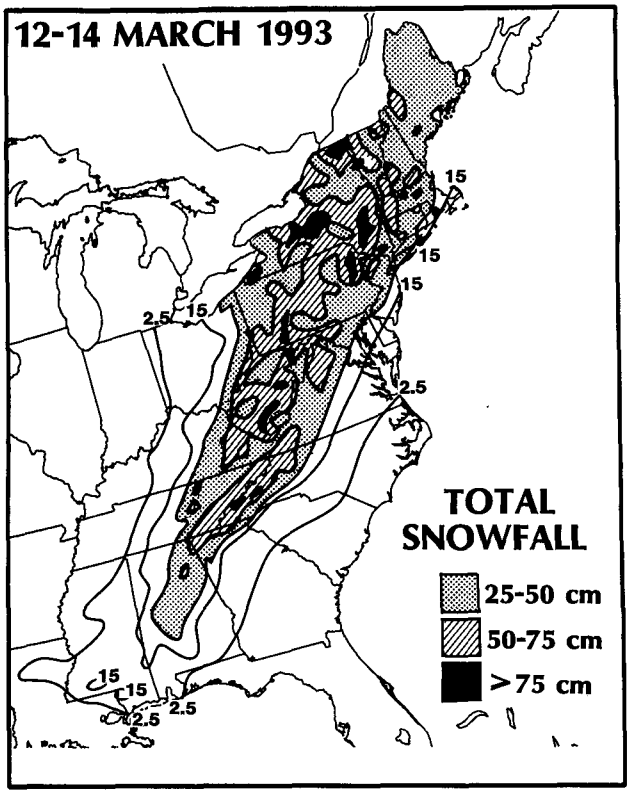

FIG. 1. Snowfall distribution (cm) for the 12–14 March superstorm.

Other factors contributed to the superstorm's severity, including severe weather and coastal flooding in Florida, flooding in Cuba, and tornadoes in extreme northeastern Mexico. According to a United Nations report, coastal flooding in Cuba was responsible for damage estimated at $1 billion, and tornadoes in extreme northeastern Mexico resulted in loss of life. At least 47 lives were lost in Florida, and damage estimates exceed $1.6 billion. Eleven confirmed tornadoes were responsible for seven deaths in Florida as a squall line swept eastward between 0400 and 0700 UTC 12 March (Fig. 2). Coastal flooding along the western Florida coastline was responsible for at least 13 fatalities and was associated with a 1.5- to 4-m storm surge that followed the passage of the storm's cold front at 0900 UTC (Fig. 2). The flooding occurred as increasing southerly winds ahead of the developing cyclone caused water levels to rise along the western Florida coast. Strong westerly gales behind the cold front caused water levels to rise rapidly after frontal passage. The persistence of the westerly gales then had the effect of maintaining high water across western Florida well after the front had passed, prolonging flooding conditions. The maximum height of the surge

[1]The precipitation distribution reported from the rain gauge network is not shown since some large discrepancies between melted precipitation measurements from rain gauges and water equivalent amounts derived from core sample measurements at selected sites have been reported (Lott 1993). It has been shown that use of gauge measurements in snowstorms accompanied by strong winds can result in significant undermeasurement of frozen precipitation (Larsen and Peck 1974). Since much of the precipitation generated in the superstorm fell as snow or ice pellets and was accompanied by strong winds, the precipitation distribution in the storm may have been significantly underrepresented.

was found in northwestern Florida, just east of the point where the surface low made landfall, where water levels were estimated at between 10 and 12 ft (3 to 4 m) above mean sea level. Along the coast of western Florida, water levels were generally between 5 and 7 ft (1.5 to 2 m) above mean sea level and subsided slowly as westerly winds diminished late on 13 March.

The storm was also notable for several other effects. For portions of the Southeast and Middle Atlantic, sea level pressures were the lowest on record along the track of the cyclone. Although numerical model forecasts indicated that the storm would undergo its greatest deepening over the Middle Atlantic and Northeast on 13 March, the storm underwent explosive deepening over the Gulf of Mexico and the Southeast on 12 March, setting numerous minimum sea level pressure records from Georgia to New York. The advection of very cold air to the Gulf Coast following the storm, combined with the extensive snow cover, resulted in numerous record-low temperatures, including 2°F (–16°C) at Birmingham, Alabama. Finally, high winds to the north and northwest of the cyclone center, both in the Gulf of Mexico as the cyclone was intensifying rapidly, and along the East Coast, as the storm was moving to the northeast, were another major component of the storm. A listing of selected record sea level pressures, record-low temperatures, and maximum wind gusts for the United States are provided in Table 1, as derived from data provided from the National Climatic Data Center.

3. Synoptic overview

The synoptic overview focuses on weather conditions during the period between Thursday evening, 0000 UTC 12 March 1993, and Sunday morning, 1200 UTC 14 March 1993, using surface weather analyses, 850-mb analyses, 500-mb charts with upper-level jets superimposed (Figs. 3, 4, and 5), infrared satellite imagery (Fig. 6), and analyses of the potential vorticity (Figs. 7 and 8).

a. Surface and upper-level analyses

1) 12 March 1993

The surface weather analysis at 0000 UTC 12 March (Fig. 3a) shows a broad region of high pressure extending across much of the northern United States with the precursor of the storm marked by a disorganized area of low pressure located south of Texas. At this time, a region of midlevel cloudiness (Fig. 6a) was associated with mostly light snows over the central Rockies and some developing showers and thundershowers over Texas, Louisiana, and Mississippi. The rainfall was developing within a low-level (850 mb) southerly airstream (Fig. 3b) near the Gulf of Mexico downwind of an upper-level trough moving eastward from the southwestern United States and northern Mexico (Fig. 3c). The cold air encompassing much of the eastern United States is indicated by the southward extension of the 0°C 850-mb isotherm to the northern Gulf states (Fig. 3b). Northwesterly flow and cold-air advection were apparent across much of the eastern United States at 850 mb, providing the low-level conditions necessary for snow. At the 500-mb level (Fig. 3c), a broad region of confluence extended over much of the eastern United States. This confluence was located upwind of an upper trough over eastern Canada associated with a cyclone moving east of Nova Scotia, and a 60 m s^{-1} upper-level jet streak over the Middle Atlantic. Upper-level confluence is an important feature for many East Coast snowstorms (Kocin and Uccellini 1990) since it acts to maintain the cold air and anticyclone over the Northeast, a requirement for the precipitation to fall as snow rather than rain along the coast.

Between 0000 and 1200 UTC 12 March, the surface low pressure area over northern Mexico consolidated into an intensifying low pressure center over the western Gulf of Mexico (Fig. 3d). Satellite imagery indicated that two regions of thunderstorms devel-

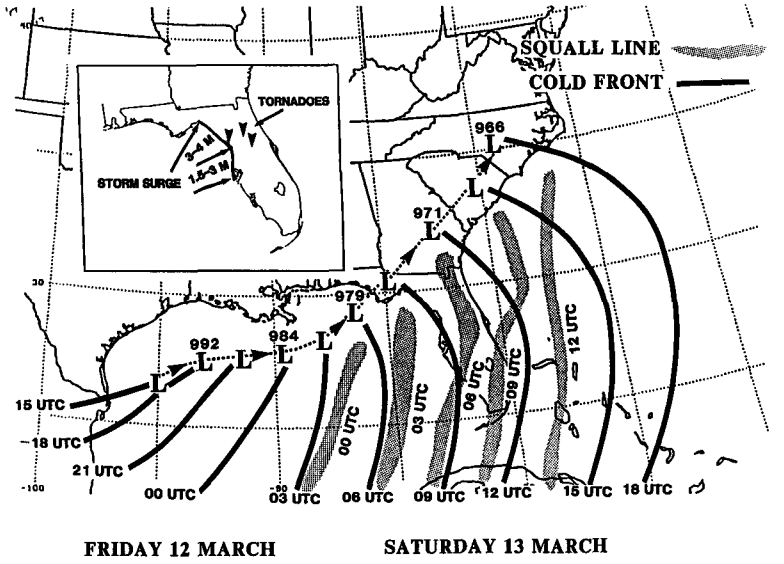

FIG. 2. The 3-hourly evolution of the locations of the surface low pressure center (L; central sea level pressures in mb are indicated every 6 h), the surface cold front (solid black line), and the squall line (shaded) on 12–13 March 1993. Inset map marks locations and depth (m) of the storm surge and approximate locations of tornado outbreak.

TABLE 1. List of record-low sea level pressures (inches; kPa), temperatures (°F; °C), and selected maximum wind gusts for the United States (mph; m s^{-1}). All sea level pressures were measured on 13 March. All temperatures occurred on 14–15 March, and all wind reports occurred on 13 March (except for South Timbalier and South Marsh Island, Louisiana, which occurred on 12 March).

Record-low sea level pressures	Inches	kPa
White Plains, NY	28.38	96.11
Philadelphia, PA	28.43	96.24
New York (JFK), NY	28.43	96.24
Dover, DE	28.45	96.30
Boston, MA	28.51	96.50
Augusta, ME	28.53	96.57
Norfolk, VA	28.54	96.60
Washington, DC	28.54	96.60
Raleigh, NC	28.61	96.86
Columbia, SC	28.63	96.93
Augusta, GA	28.73	97.30
Greenville–Spartanburg, SC	28.74	97.34
Asheville, NC	28.89	97.84

Highest recorded wind gusts	mph	(m s^{-1})
Mount Washington, NH	144	(64.4)
Dry Tortugas, FL	109	(48.7)
Flattop Mountain, NC	101	(45.2)
South Timbalier, LA	98	(43.8)
South Marsh Island, LA	92	(41.1)
Myrtle Beach, SC	90	(40.2)
Fire Island, NY	89	(39.8)
Vero Beach, FL	83	(37.1)
Boston, MA	81	(36.2)
LaGuardia Airport, NY	71	(31.7)

Record-low temperatures	°F	°C
Burlington, VT	−12°	−24.4°
Caribou, ME	−12°	−24.4°
Syracuse, NY	−11°	−23.9°
Mount LeConte, TN	−10°	−23.3°
Elkins, WV	−5°	−20.6°
Waynesville, NC	−4°	−20.0°
Rochester, NY	−4°	−20.0°
Pittsburgh, PA	1°	−17.2°
Beckley, WV	1°	−17.2°
Asheville, NC	2°	−16.7°
Birmingham, AL	2°	−16.7°
Knoxville, TN	6°	−14.4°
Greensboro, NC	8°	−13.3°
Chattanooga, TN	11°	−11.6°
Philadelphia, PA	11°	−11.6°
New York, NY	14°	−10.0°
Washington, DC	15°	−9.4°
Montgomery, AL	17°	−8.3°
Columbia, SC	18°	−7.8°
Atlanta, GA	18°	−7.8°
Augusta, GA	19°	−7.2°
Mobile, AL	21°	−6.1°
Savannah, GA	25°	−3.9°
Pensacola, FL	25°	−3.9°
Daytona Beach, FL	31°	0.0°

oped rapidly over the south Texas–Mexican border and off the southern Texas coast. These two regions then merged into the rapidly expanding region of cold cloud tops over southern Texas and the western Gulf of Mexico, while a region of relatively colder upper-level clouds began to stream northeastward through the Tennessee Valley (Fig. 6b). Water vapor imagery (not shown) indicated that a significant region of midtropospheric dryness accompanied the thunderstorm development near the Texas–Mexican border. At the surface, cold air across northern Texas rushed southward into southern Texas coincident with the development of the thunderstorms. While light snow fell across the panhandles of Texas and Oklahoma into Colorado, ice pellets and snow developed along the northern edge of the expanding precipitation shield across northern Louisiana and western Mississippi. The developing 850-mb circulation at 1200 UTC (Fig. 3e) was collocated along the warm edge of the lower-tropospheric baroclinic zone and was associated with an expanding area of radar echoes with VIP (video integrator and processor) levels greater than 2 over the western Gulf of Mexico. The rain/snow boundary was collocated with the 850-mb 0°C isotherm in northern Louisiana, which continued to drift southward overnight in Alabama and points west. Farther east, the 850-mb 0°C contour remained virtually stationary over South and North Carolina.

At 500 mb (Fig. 3f), the trough over Nova Scotia, confluent flow extending across the northeastern United States, and a dual-trough system developing across the central and south-central United States (indicated by separate vorticity maxima over Colorado and just south of Texas) remained the key features, similar to

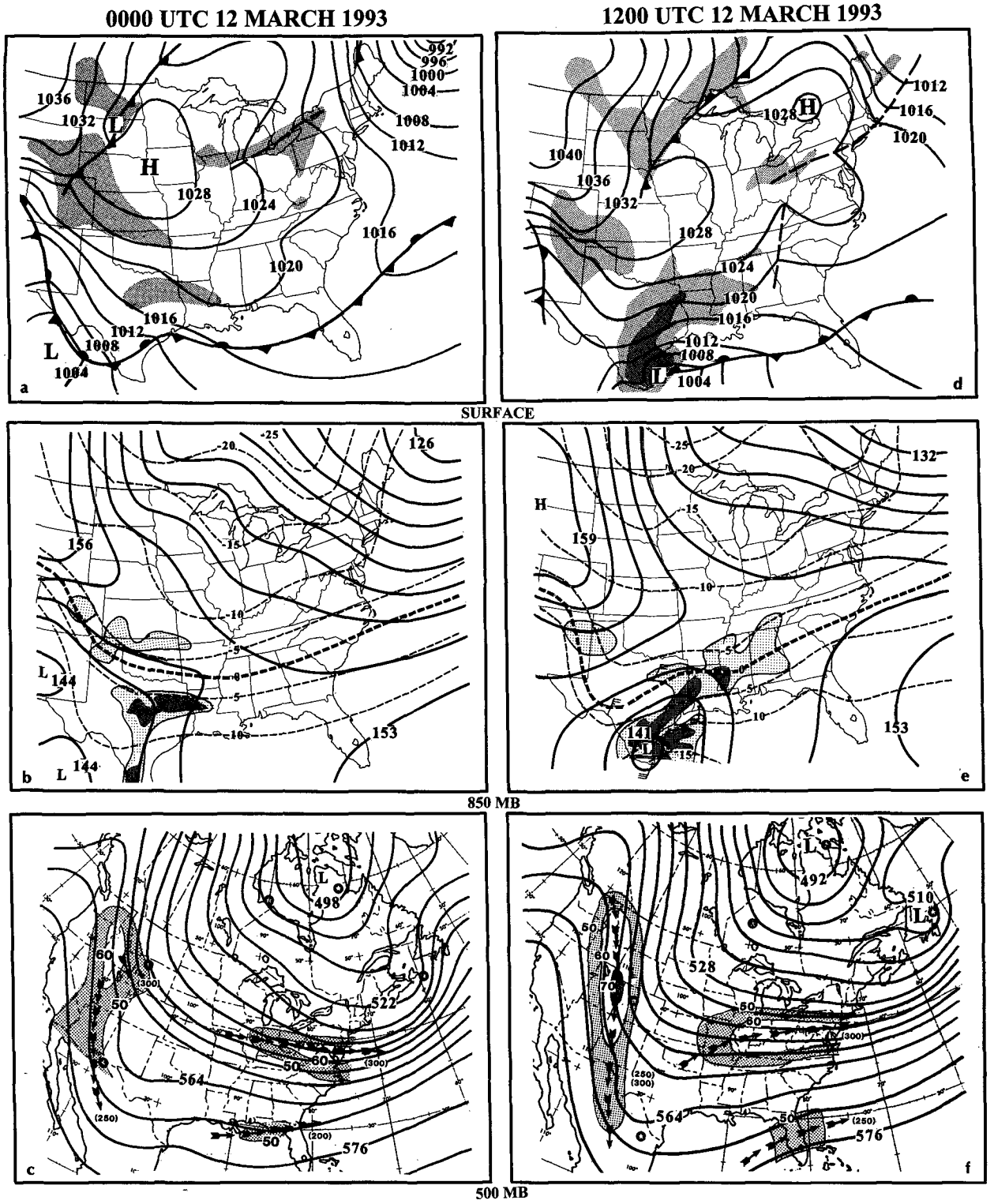

FIG. 3. Surface, 850-mb, and upper-level analyses for 0000 (left) and 1200 UTC (right) 12 March 1993. Surface maps include surface high and low pressure centers and fronts; shading indicates precipitation (heavy shading denotes moderate to heavy precipition), solid lines are isobars (4-mb increments), and dashed lines represent axes of surface troughs not considered to be fronts. The 850-mb maps include contours of geopotential height (solid, at 30-m intervals, 156 = 1560 m) and isotherms (dashed, °C, 5°C intervals); shading represents manually digitized radar video integrator and processor (VIP) echoes (embedded shading represents VIP levels greater than 2). Upper-level analyses include contours of 500-mb geopotential height (solid, at 60-m intervals, 522 = 5220 m), locations of 500-mb absolute vorticity maxima (circled stars), axes of upper-level wind maxima (arrows), and composite isotachs of maximum wind speeds derived from either the 500-, 300-, 250-, or 200-mb levels (values in parentheses represent level of maximum wind speed); alternating intervals of shading represent 10 m s^{-1} increments in wind speed.

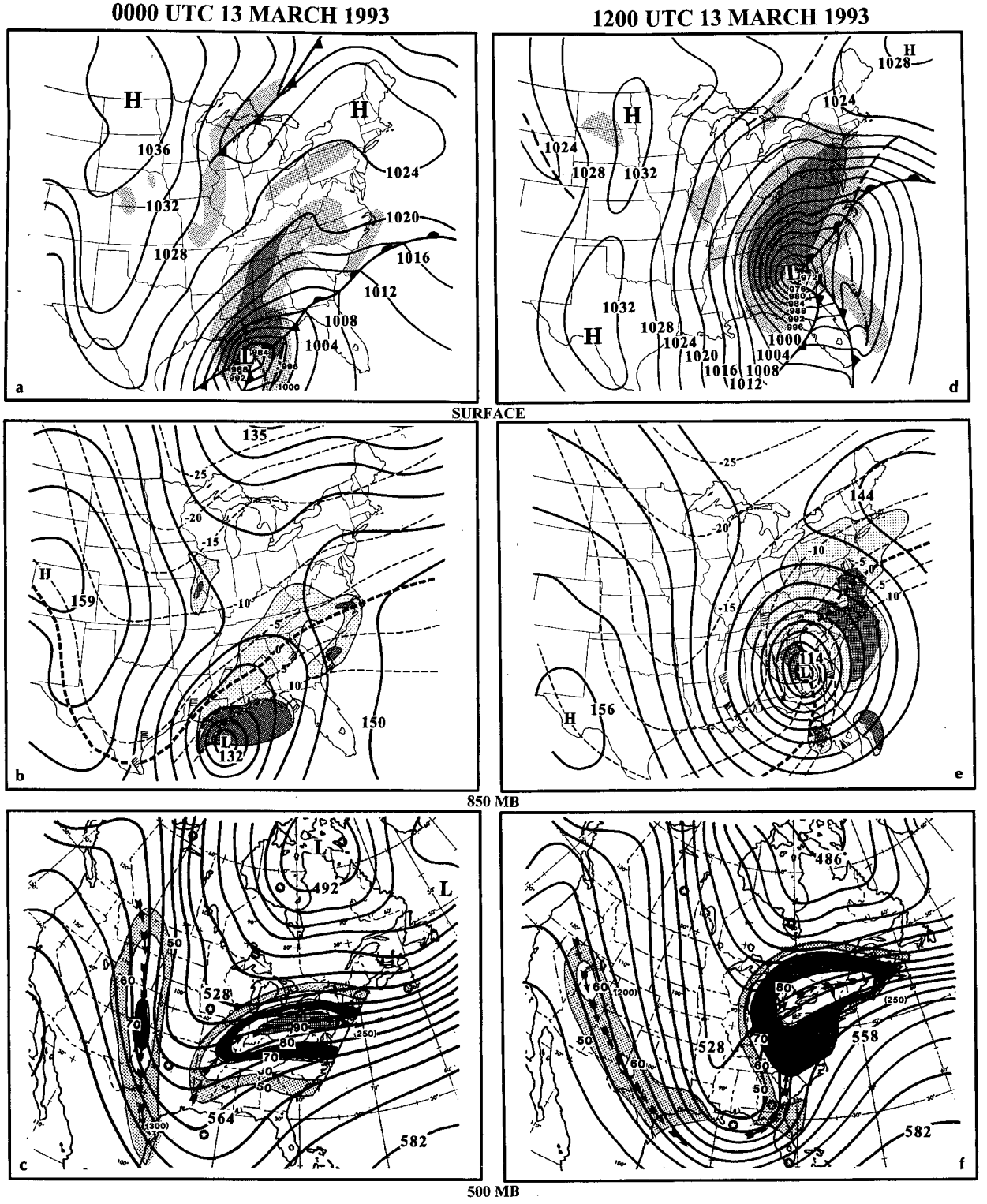

FIG. 4. Surface, 850-mb, and upper-level analyses for 0000 (left) and 1200 UTC 13 March 1993. See Fig. 3 for details.

the upper-air patterns observed prior to numerous major East Coast snowstorms (Kocin and Uccellini 1990). Two separate jet streaks are clearly analyzed during the precyclogenetic period. One jet streak with maximum winds exceeding 60 m s^{-1} at 300 mb was associated with the confluent flow over the northeastern United States and extended from the Ohio Valley to the Middle Atlantic coast. The other jet streak was

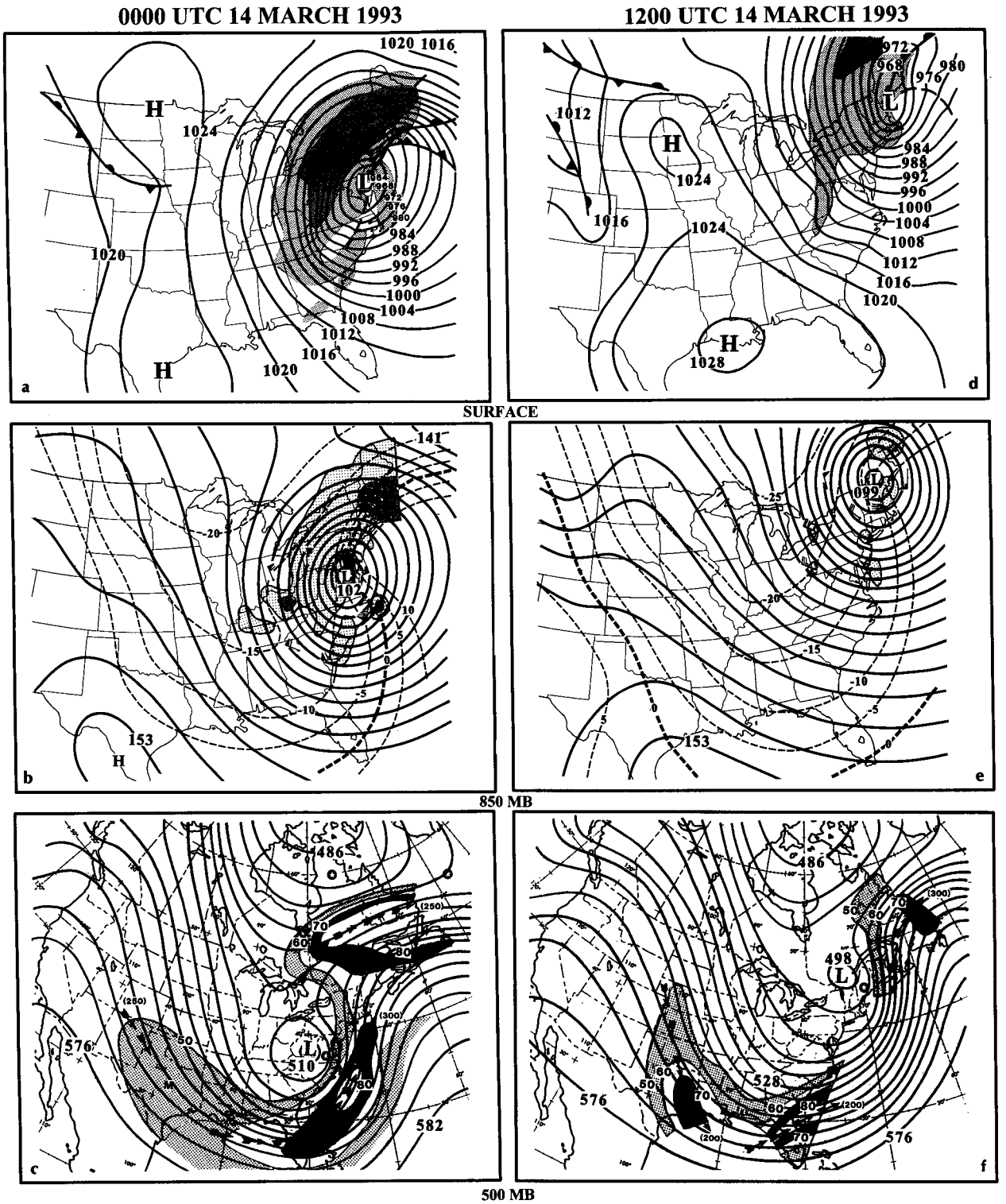

FIG. 5. Surface, 850-mb, and upper-level analyses for 0000 (left) and 1200 UTC 14 March 1993. See Fig. 3 for details.

associated with the dual-trough system and was located over the western United States with maximum winds of 70 m s^{-1} at 250 mb.

The cyclone moved progressively east-northeastward over the Gulf of Mexico and deepened 17 mb in 12 h to reach a central pressure estimated at 984 mb south of Louisiana at 0000 UTC 13 March (Fig. 4a), a rate of intensification that is rarely observed over the

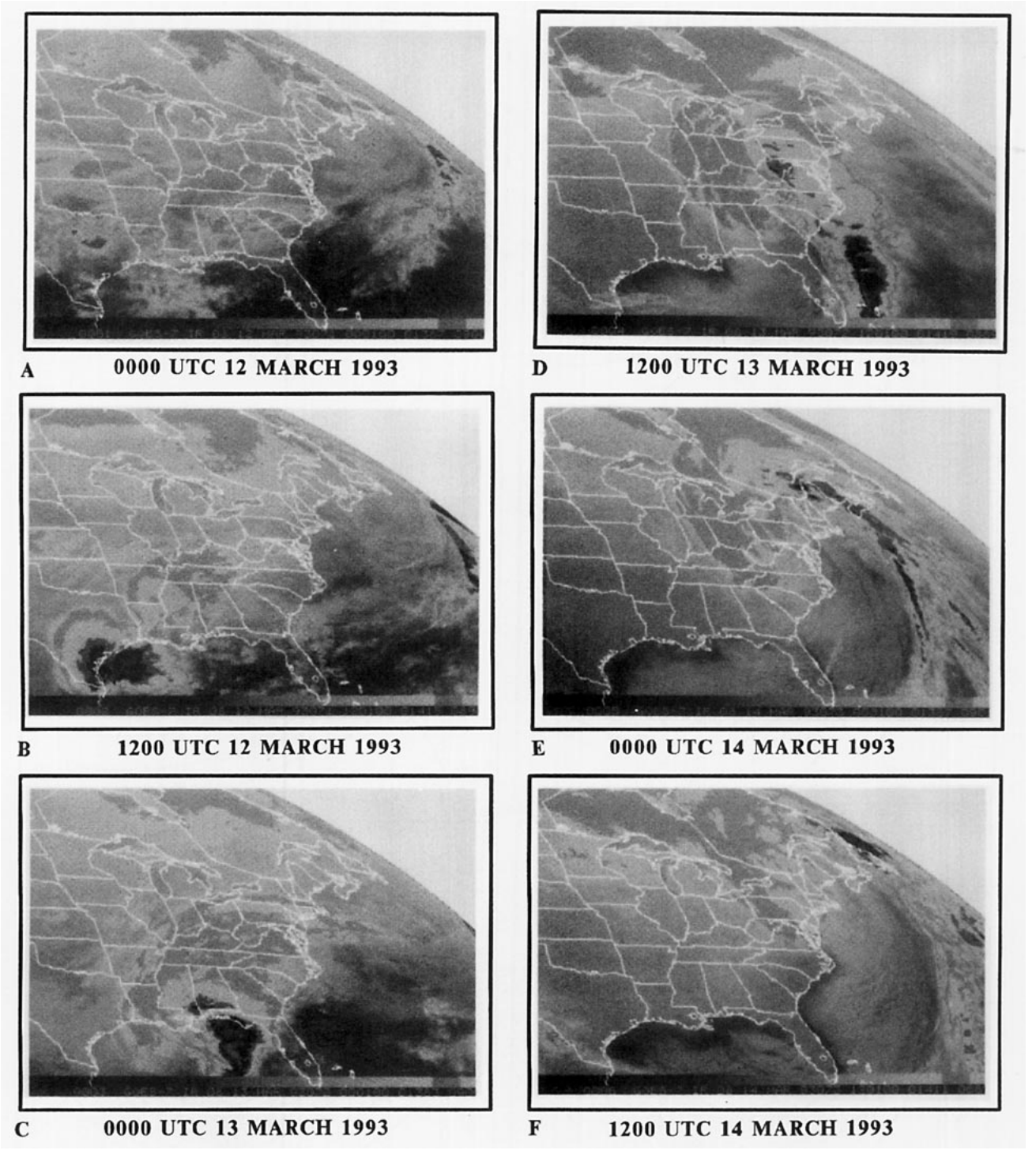

FIG. 6. The 12-hourly infrared satellite images for 0000 UTC 12 March through 1200 UTC 14 March 1993.

Gulf of Mexico for an extratropical cyclone. The cyclone was associated with a squall line and complex frontal structure, which will be documented in more detail in section 4. To the north and northwest of the cyclone center, hurricane-force winds were observed from ships and oil rig platforms while warm, humid air with dewpoints near 20°C moved northward over Florida. At 0000 UTC 13 March, a strong frontal boundary over northern Florida and south-central Georgia provided an early indication of where the surface cyclone would later make landfall. Heavy rainfall and thunderstorms developed from Louisiana

to northwestern Florida, while snowfall expanded from southern Mississippi northeastward across the eastern Tennessee Valley, into West Virginia, western Virginia, and North Carolina. Snowfall accumulations were still relatively light. Satellite imagery (Fig. 6c) shows a well-defined comma-shaped cloud circulation and intense convection over the Gulf of Mexico, and relatively cold upper clouds continuing to stream northeastward into the northeastern United States. Above the surface, a well-defined 850-mb circulation was located south of Louisiana (Fig. 4b), still considerably south of the 0°C isotherm, with the expanding region of radar echoes aligning with the southwest–northeast-oriented baroclinic zone. The temperature gradient surrounding the 0°C isotherm was increasing, consistent with the frontogenesis implied by the 30-kt southeasterly wind at Appalachicola, Florida, and the 15-kt northeasterly wind at Centreville, Alabama.

Some dramatic changes in the upper-level height and wind fields were observed at 0000 UTC 13 March (Fig. 4c). Perhaps the most dramatic change was the increasing wind speeds within the upper-level jet streak over the Ohio Valley and the northeastern United States. As the cyclone developed rapidly over the Gulf of Mexico, maximum winds in this jet increased over 30 m s^{-1} in 12 h. This increase occurred at the crest of an amplifying ridge over the southeastern United States, coincident with the intense latent heat release associated with the strong convection over the Gulf of Mexico. Similar intensifications of the downstream jet streak have been documented for other cases of rapid cyclogenesis (see, e.g., Chang et al. 1982; Keyser and Johnson 1984; Uccellini 1991).

2) 13 March 1993

Following 0000 UTC 13 March, the cyclone continued to move northeastward and intensify, reaching the northwest coast of Florida around 0800 UTC, passing just to the west of Tallahassee. A squall line, accompanied by numerous severe thunderstorms and at least 11 tornadoes, swept across Florida between 0400 and 0700 UTC (Fig. 2). The squall line was located to the east of the main cold front, which reached the west coast of Florida around 0900 UTC. It appears that coastal flooding reached a depth of 10 to 12 ft (3 to 4 m) along the northwestern coast of Florida from east of Tallahassee to north of Tampa Bay (Fig. 2). The peak of the flood occurred with the passage of the surface cold front over a relatively narrow region just to the east of the point where the surface low made landfall in northwestern Florida. However, flooding was also a problem for much of western Florida and the northern coast of Cuba.

The cyclone continued to deepen as the central pressure fell an additional 12 mb to 971 mb over southeastern Georgia at 1200 UTC 13 March (Fig. 4d). Colder air rushed in behind the cyclone and rain changed to snow as far south as the Gulf Coast and northern Florida. To the north of the center, snow continued to spread northward into the Middle Atlantic states, eastern Kentucky, and Ohio, and into extreme southern New England by 1200 UTC. Snowfall rates increased dramatically overnight across eastern Mississippi, northern Alabama, and eastern Tennessee, and moderate to heavy snows also developed across West Virginia, Virginia, Maryland, Pennsylvania, and New Jersey. Satellite imagery (Fig. 6d) shows that an expansive comma-shaped cloud shield with intense convection was located well east of the Florida coast with the comma head associated with the heavy snowfall located over Tennessee, Alabama, and Georgia.

The 850-mb analysis at 1200 UTC 13 March (Fig. 4e) shows that a massive circulation developed in the lower troposphere over the southeastern United States, accompanied by an increase in the temperature gradients along the baroclinic zone in northern Florida, eastern Georgia, and the Carolinas, and an increase of observed wind speeds (for those stations still reporting winds) surrounding the cyclone. In addition, the 850-mb low center became collocated with the 0°C isotherm with strong warm-air advection located northeast of the center and strong cold-air advection to the south. The 0°C to -2°C isotherm corresponds closely to the rain/snow line, with the greatest VIP levels found in the southeasterly 850-mb flow from the Atlantic Ocean to North Carolina and into the Middle Atlantic states as moisture-laden air in the warm sector of the cyclone ascends over the colder air west of the coastline. A secondary area of higher reflectivities is found near and immediately west of the cyclone center in Georgia where rain was changing over to heavy snow. At 500 mb (Fig. 4f), the upper troughs have merged into a highly amplified, negatively tilted trough characterized by very strong height falls [–290 m $(12\ h)^{-1}$ at Waycross, Georgia]. A highly confluent region over the northeastern United States is associated with the strong jet streak that shifted northward and maintained maximum wind speeds near 90 m s^{-1}.

Following 1200 UTC 13 March, the cyclone center moved northeastward along the eastern seaboard, crossed the central portions of South and North Carolina, eastern Virginia, and the Chesapeake Bay, and was located over Delaware by 0000 UTC 14 March (Fig. 5a). The cyclone had deepened another 11 mb, reaching its minimum value of 960 mb at this time. Heavy snow fell throughout much of the Southeast, across the Appalachians, the Middle Atlantic states, and New England. High winds accompanied the heavy snow with temperatures primarily in the 20s to lower

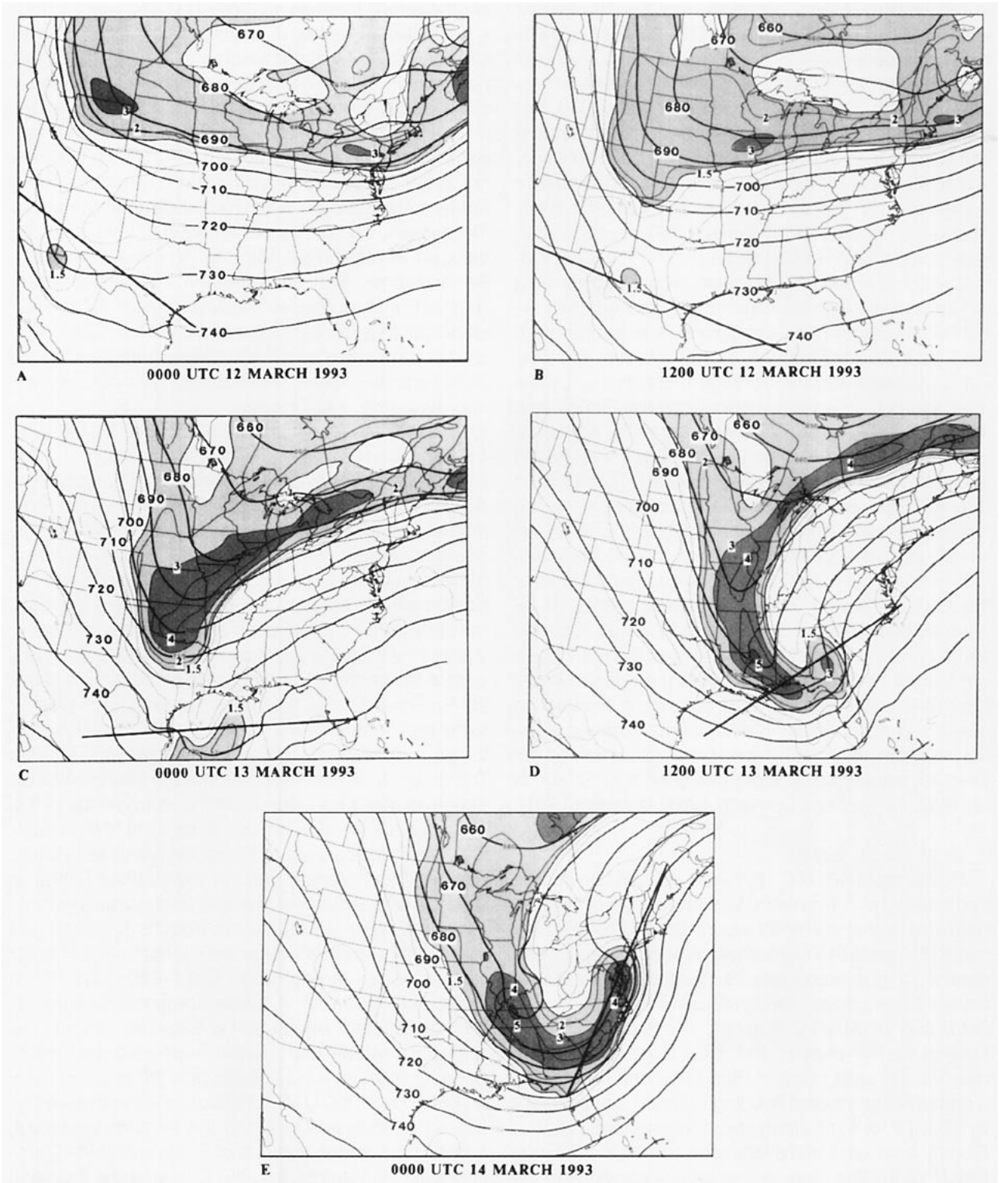

FIG. 7. The 12-hourly analyses of 400-mb geopotential heights (solid, 740 = 7400 m) and 500–300-mb mean-layer potential vorticity ($2 = 2 \times 10^{-5}$ K mb^{-1} s^{-1}; shading for values greater than 1.5×10^{-5} K mb^{-1} s^{-1}; heavy shading for values greater than 3×10^{-5} K mb^{-1} s^{-1}) for 0000 UTC 12 March through 1200 UTC 14 March 1993. Thick black line represents axis of cross sections shown in Fig. 8.

30s °F (–7° to 0°C) during the initial phase of the storm for much of the region, but fell into the teens and 20s °F (–10° to –5°C) later in the day. The storm's slightly inland track prevented excessive accumulations of snow in the heavily populated urban corridor as snow changed to ice pellets and then briefly to rain. Some of

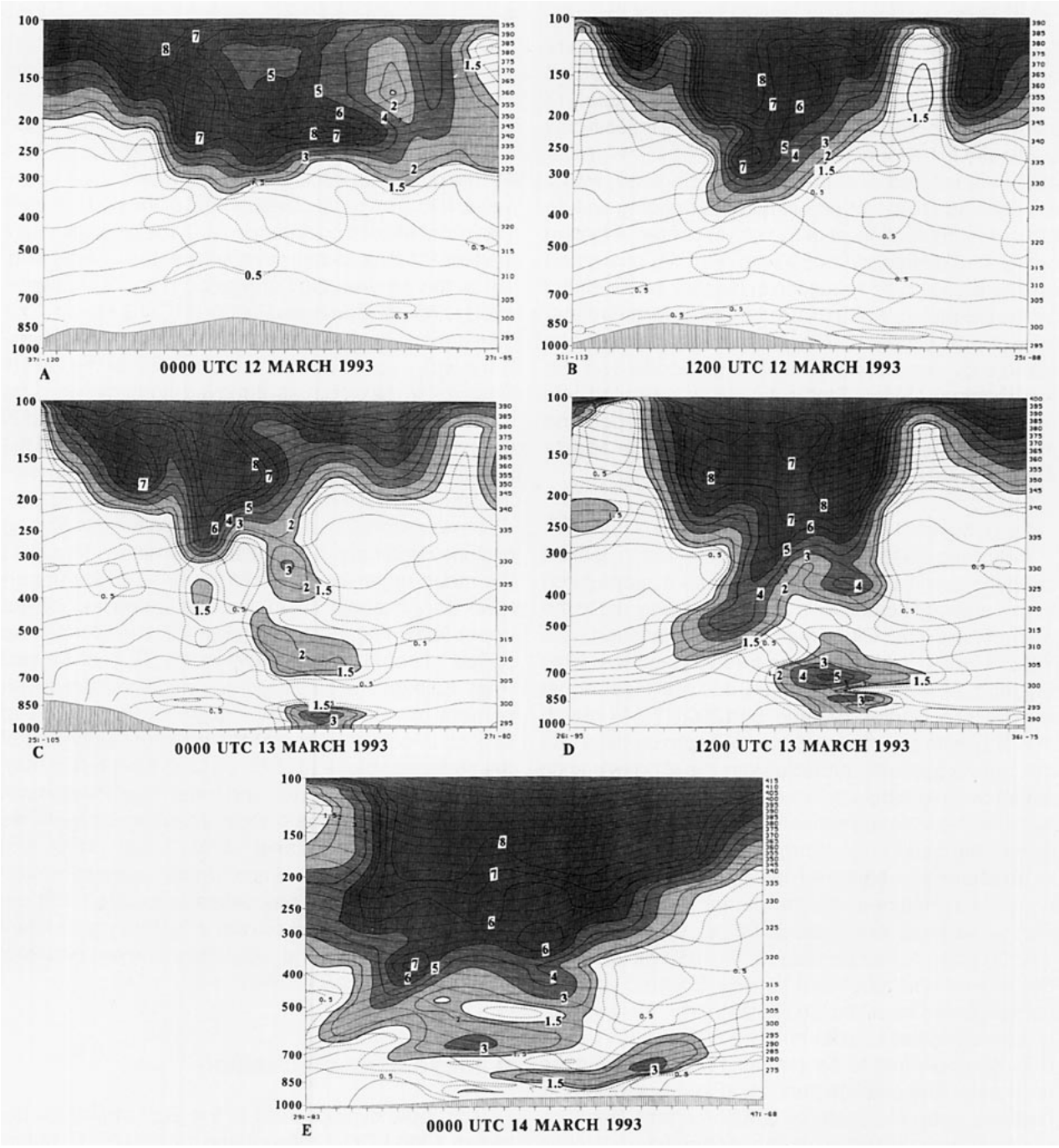

FIG. 8. Vertical cross sections oriented through surface cyclone and parallel to upper-level flow for 0000 UTC 12 March through 1200 UTC 14 March 1993, including isentropes (solid, K) and potential vorticity (dashed and shaded; $1.5 = 1.5 \times 10^{-5}$ K mb^{-1} s^{-1}; solid contours and shading for values exceeding 1.5×10^{-5} K mb^{-1} s^{-1}; heavy shading for values greater than 3×10^{-5} K mb^{-1} s^{-1}).

the strongest winds observed during the storm appeared to occur during the period when heavy snow changed to heavy ice pellets. Wind speeds approached hurricane force for a brief period of time along the immediate coastline and were accompanied by sea level pressure falls approaching 20 mb (3 h)$^{-1}$. Satellite imagery (Fig. 6e) shows that the cloud mass was marked by a region of relative lower-level dryness that raced northeastward and extended well to the northeast of the surface low pressure center. The comma-shaped tail moved out over the Atlantic Ocean with diminishing colder tops, indicative of weakening convection, while a broad comma-shaped head was located over the Middle Atlantic and Ohio Valley states.

The 850-mb low center at 0000 UTC 14 March (Fig. 5b) was now associated with a narrow, intense baroclinic zone near and to the northeast of the storm center with the 0°C isotherm corresponding closely to the snow/ice pellet boundary. Highest radar reflectivities continued to be found well northeast of the low center and were located over eastern New England, with a widespread region of precipitation extending well to the west and southwest of the storm center. A closed center had developed at 500 mb (Fig. 5c) characterized by a continued reduction in heights, as indicated by the height fall of 350 m $12h^{-1}$ measured at Greensboro, North Carolina. The jet streak that had been marked by exceptionally high wind speeds over the northeastern United States had now retreated into eastern Canada as the upper vortex developed and moved northeastward to a position over the Middle Atlantic states.

3) 14 March 1993

Following 0000 UTC 14 March, the storm ceased deepening and began to fill slowly as it propagated from Delaware across New Jersey, passing just to the west of New York City. Once the center passed New York, it took a slight right turn through southern New England, passed west of Boston, and was located just to the east of Portland, Maine, by 1200 UTC 14 March (Fig. 5d), with a central pressure of approximately 964 mb. Snows gradually ended across the Middle Atlantic states overnight but continued across much of Pennsylvania, New York, interior New England, and Maine. Snow changed to rain along the immediate coastline of southern and eastern New England, but blizzard conditions remained over the interior of New York and Pennsylvania as temperatures fell below 10°F (−14° to −12°C) in the higher elevations. The 850-mb low (Fig. 5e) moved northeastward to New England and became located near the −10°C isotherm, moving progressively toward colder air. The 500-mb low center (Fig. 5f) continued to deepen as it propagated to the northeast. The satellite imagery (Fig. 6f) shows only portions of an increasingly diffuse comma head remaining over sections of the northeastern United States. Following 1200 UTC 14 March, the cyclone continued moving northeastward, exiting the United States by 1800 UTC. The snowfall gradually ended across New England, followed by clearing skies and below-freezing temperatures.

b. Potential vorticity perspective

An analysis of the 500–300-mb layer-average potential vorticity (PV) indicated two distinct potential vorticity maxima involved with the March 1993 superstorm (Fig. 7). The maxima were associated with separate short-wave systems that merged over the Southeast during the intense cyclogenesis. The 500–300-mb layer was chosen to highlight the PV anomaly that descended into the layer initially associated with the upper troposphere. Amplification of the layer-average PV was associated not only with nonadiabatic processes, but also with adiabatic descent of the PV maximum as occurs in association with a tropopause fold. The rapid development of the cyclone over the Gulf of Mexico commenced with the propagation of the first PV maximum from southwestern Texas (Fig. 7b) to the western Gulf of Mexico (Fig. 7c) between 1200 UTC 12 March and 0000 UTC 13 March. The subsequent development and movement of the cyclone was marked by 1) an amplification of the Gulf of Mexico PV maximum as it moved northeastward toward the southeastern United States (Fig. 7d), and 2) the expansion of the northern PV maximum toward the Gulf of Mexico (Fig. 7c) and its apparent merger with the southern system by 0000 UTC 14 March (Fig. 7e).

Cross sections constructed through the developing cyclone center and oriented approximately parallel to the mean upper-level flow at the base of the upper-level trough show the downward extension of the upper-level PV maximum prior to and during the period of rapid cyclogenesis in the Gulf of Mexico (Figs. 8a,b,c). The cross sections also show the development of a low-level PV maximum in the Gulf of Mexico in conjunction with the rapid development of the surface cyclone at 0000 UTC 13 March (Fig. 8c). The interactions of upper- and lower-level PV maxima have been noted for other rapidly developing cyclones (Gyakum 1983; Whitaker et al. 1988; Davis and Emanuel 1991) and are known to be diagnostic markers for the interactive processes associated with upper-level jet streaks/short-wave features and latent heat release during the rapid development phase of the cyclone (Uccellini 1991).

4. Mesoscale discussion

The rapid cyclogenesis in the Gulf of Mexico between 1200 UTC 12 March and 1200 UTC 13 March was poorly predicted by the numerical models (Caplan 1995). The cyclone deepened from 1000 to 971 mb in 24 h, over 10 mb deeper than any model forecast initialized at 1200 UTC 12 March 1993. This unexpected strengthening resulted in very strong winds to the north and west of the cyclone center as well as an unprecedented storm surge along the Florida and Cuba coasts. While the precise mechanisms for the earlier than expected rapid cyclogenesis are beyond the scope of this paper, the evolution of the surface cyclone during this period and the associated frontal structures are discussed.

To provide an accurate depiction of the cyclone evolution over the Gulf of Mexico, several sources of data were used. The primary source of surface observations was the GEMPAK[2] files, which consisted of data ingested from the Domestic Data Service line at the NMC. These observations were supplemented by paper copies of first-order, cooperative, and U.S. Coast Guard reports obtained from the National Climatic Data Center (NCDC) in Asheville, North Carolina. Furthermore, ship, buoy, and C-MAN (Coastal-Marine Automated Network) data were obtained in raw form from the State University of New York at Albany, and were supplemented by paper copies of buoy and C-MAN data obtained from the National Buoy Data Center. In addition to observations, infrared satellite imagery and composite radar depictions of the eastern Gulf of Mexico were used to enhance the analyses in data-sparse areas.

Pressure and temperature were subjectively analyzed for each hour. Because data were sparse in the Gulf of Mexico, time series of temperature, pressure, and wind were used to help identify the approximate speed and location of the fronts, troughs, and squall line. In addition, satellite and radar signatures were tracked to aid in the positioning of fronts and troughs in data-sparse areas. Finally, after all the analyses were completed, the positions of both the cyclone and the fronts were cross checked to ensure a smooth, consistent rate of propagation.

a. Surface cyclone evolution

At 1200 UTC 12 March 1993, a 1000-mb cyclone was located just off the Texas coast, near Corpus Christi (Fig. 3d). An asymmetry in the cyclone structure was evident with a much tighter pressure gradient located to the north and west of the cyclone. The cyclone began to deepen at approximately 1.5 mb h^{-1} after 1500 UTC with the central pressure falling to 992 mb by 1800 UTC (Fig. 9a). Coincident with the rapid deepening, the pressure gradient increased significantly north of the storm. Wind reports from oil rigs off the Louisiana coast were over 25 m s^{-1} directed from the northeast, with a maximum of 35 m s^{-1} recorded at 2100 UTC (Fig. 9b). This strengthening allowed cold, dry air to be advected rapidly southward into Mississippi and Alabama.

During the next 6 h, the storm continued to deepen at a rate of 1.5 mb h^{-1} and reached a central pressure of 984 mb at 0000 UTC 13 March (Fig. 9c). The cyclonic circulation around the storm had expanded to cover the southeastern quarter of the United States, and precipitation associated with the storm extended northward into western Pennsylvania (Fig. 4a). During this period, a large outbreak of convection was observed near the cyclone (see Figs. 6b,c). The advection of cold air over the Gulf at midlevels (not shown) may have supported the development of the convection by reducing the static stability. This convection, through latent heating, may have contributed to the strengthening of the downstream jet (Fig. 4c) and the unforecast rapid deepening of the cyclone in a manner that has been described for other cyclones by Chang et al. (1982), Uccellini (1991), and others.

Between 0000 and 0600 UTC 13 March, the rate of intensification appeared to decrease to approximately 1 mb h^{-1} as the storm turned northeastward toward the Florida panhandle. The asymmetry in the cyclone structure remained evident as the storm moved northeastward between 0000 and 0300 UTC (Fig. 9d), with the pressure gradient in the northwest quadrant of the storm continuing to strengthen with winds of greater than 15 m s^{-1} observed on the Louisiana coast. Northeast of the storm and north of the stationary front, the pressure gradient was weaker with winds less than 10 m s^{-1}. As the cyclone made landfall, it continued to deepen at 1 mb h^{-1}. A pressure trace from Tallahassee, Florida (Fig. 10), just east of the cyclone center at 0900 UTC (Fig. 9f), showed a rapid pressure fall and rise centered on the minimum pressure of 975.5 mb. This structure is similar to profiles observed with the passage of strong tropical cyclones.

Overall, the cyclone deepened 29 mb in 24 h, which was not extraordinary when compared to many rapidly deepening western Atlantic cyclones. However, when normalized for latitudinal positions, as proposed by Sanders and Gyakum (1980), this rate was 2.2 bergerons, equivalent to 52 mb in 24 h at 60°N. The asymmetric pressure distribution, coupled with the rapid deepening, resulted in extremely high winds north of the low center.

b. Surface boundaries

1) WARM/STATIONARY FRONT

The evolution of the front to the east of the cyclone is significant since the cyclone moved and developed along this boundary. In this discussion, the front will be referred to as a stationary front because of its quasi-stationary nature since to alternately refer to the front as warm and stationary would confuse the description. The stationary front extended eastward from the cyclone into the northern Gulf of Mexico at 1200 UTC 12 March and by 1800 UTC was strung across the Florida panhandle and into southern Georgia (Fig. 9a), where there had been strong frontogenesis the previous 6 h. Temperatures south of the front were near or greater

[2]The general meteorological software package (GEMPAK) was developed at the NASA/Goddard Spaceflight Center by Mary desJardins and others.

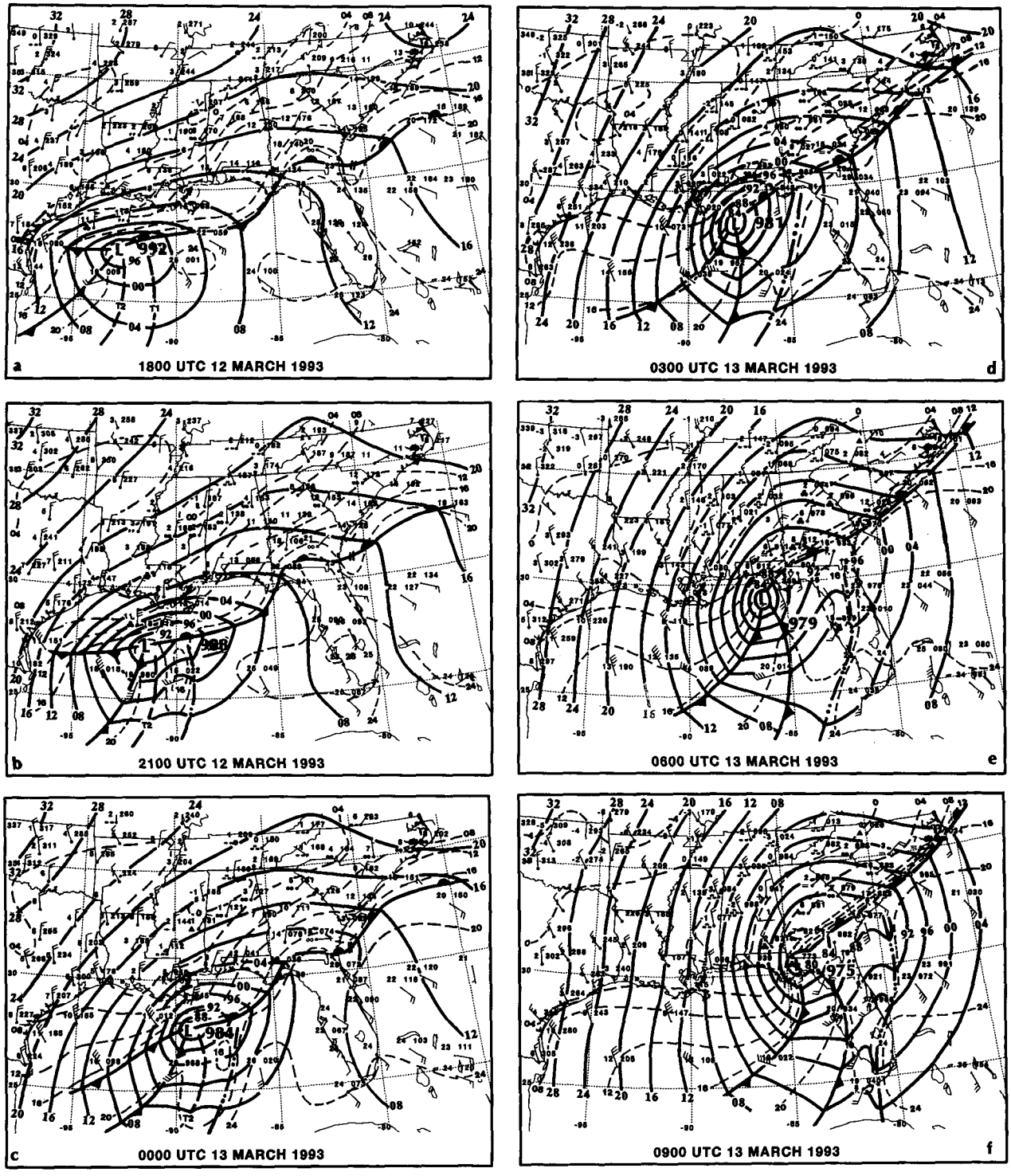

FIG. 9. Subjective surface analyses with temperature contoured every 4°C and pressure every 4 mb. Here T1 and T2 refer to the eastern and western troughs, respectively. (a) 1800 UTC 12 March 1993, (b) 2100 UTC 12 March, (c) 0000 UTC 13 March, (d) 0300 UTC 13 March, (e) 0600 UTC 13 March, and (f) 0900 UTC 13 March.

than 25°C, while north of the front they were generally between 10° and 18°C. Off the southeast coast, a coastal front formed along a weak shear axis separating colder air that was "dammed" over the continent by the northeasterly winds immediately inland of the coast, in contrast to the southeasterly flow advecting

the warmer air over the ocean toward the coastline (Figs. 9c and 9d).

In the northern Gulf of Mexico, winds south of the front were generally less than 15 m s^{-1}, while winds greater than 25 m s^{-1} were confined north of the low center. The strong acceleration of the wind north of the front may have prevented its northward movement. In fact, the front retreated slowly southward following 1800 UTC. A time series from Bullwinkle, a C-MAN station south of New Orleans, depicts a wind shift from southeast to northeast between 1800 and 2100 UTC (Fig. 11a). Its speed increased from 8 to over 20 m s^{-1} as the front moved south of the station.

Between 1800 and 0000 UTC 13 March, the front remained nearly stationary in the Gulf despite the rapid deepening of the cyclone. However, the front northeast of the storm center and especially off the southeast coast began to strengthen and move slowly westward after 1800 UTC. The temperature gradients east of the cyclone center strengthened dramatically between 0000 and 0600 UTC 13 March [Figs. 9c,d,e; similar to those observed at 850 mb as discussed in section 3a(2)]. For example, the temperature difference between Tallahassee and Dothan, Alabama (not shown), approximately 100 km apart, increased from 7° to 11°C. Farther north, the temperature difference between Wilmington, North Carolina (not shown), and Frying Pan Shoals, North Carolina (60 km apart), increased from 9° to 13°C between 0300 and 0600 UTC. The implied frontogenesis coincided with the increasing southeasterly winds in the warm air (e.g., see Fig. 9e). The increasing winds and implied increase in convergence along the coastal front likely made a significant contribution to an intensification of the low-level baroclinic zone similar to that described by Doyle and Warner (1993). Furthermore, as warm air moved northwestward toward the coastline, the temperature gradient was further strengthened because the cold-air damming effectively held the cold air in place along the coast (Bell and Bosart 1988). This implied frontogenesis preceded the northeastward movement of the cyclone along the frontal boundary.

2) Cold fronts

There were two cold fronts that were associated with the cyclone. We will refer to the leading front as the primary cold front since it was the initial frontal feature associated with the cyclone. The trailing or secondary cold front (or bent-back warm front) developed during the afternoon of 12 March and became the location of the largest temperature gradients after 0000 UTC 13 March. The primary cold front was associated with the storm surge on the west coast of Florida. The cold front was located near Brownsville,

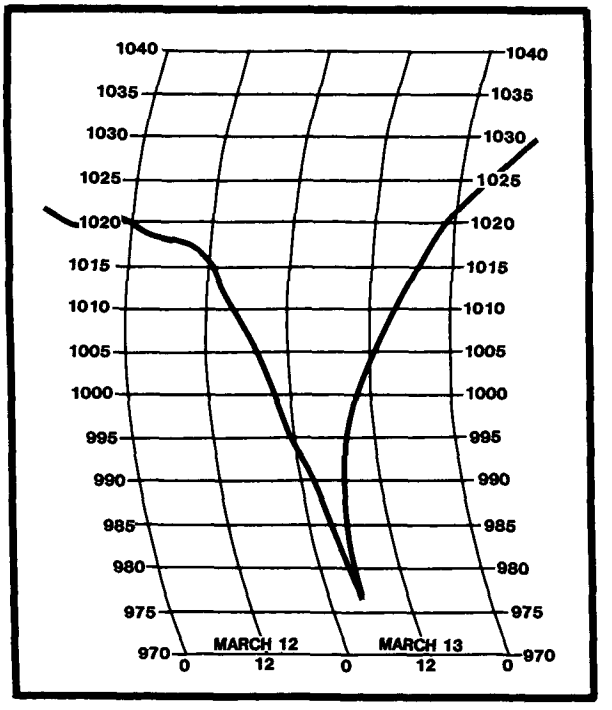

Fig. 10. Pressure trace for Tallahassee, Florida, on 12–13 March 1993. High-frequency waves have been smoothed out.

Texas, at 1200 UTC. At this time, a strong baroclinic zone extended well behind the front. During the next 6 h, the cold front moved over the Gulf of Mexico and extended southwestward toward the Mexican coast. Satellite imagery showed a lack of convection along this front. Near the low center, the temperature gradient weakened, similar to what is seen in other maritime cyclones (Shapiro and Keyser 1990). As the front continued eastward during the afternoon, the wind speed increased behind the front. As the front passed Brownsville, the wind speed increased to 10 m s^{-1}, while several hours later as the storm crossed buoy 42001, located in the western Gulf of Mexico, the wind speed increased to greater than 25 m s^{-1}. The strengthening of winds behind the front as it moved from Brownsville to the western Gulf may have been due to a combination of decreased friction over the Gulf, the rapid deepening of the storm, and the downward transport of higher-momentum air as sensible heating over the Gulf deepened the mixed boundary layer.

The sequence of a rapid 1-h temperature drop, wind shift, and dramatic increase in wind speed continued as the front moved across the Gulf of Mexico. Once the storm began to move northeastward, the cold front began to bow eastward. Southerly winds ahead of the front intensified with speeds over 20 m s^{-1} extending across the eastern Gulf of Mexico. As the front crossed the Florida coast at 0900 UTC, the

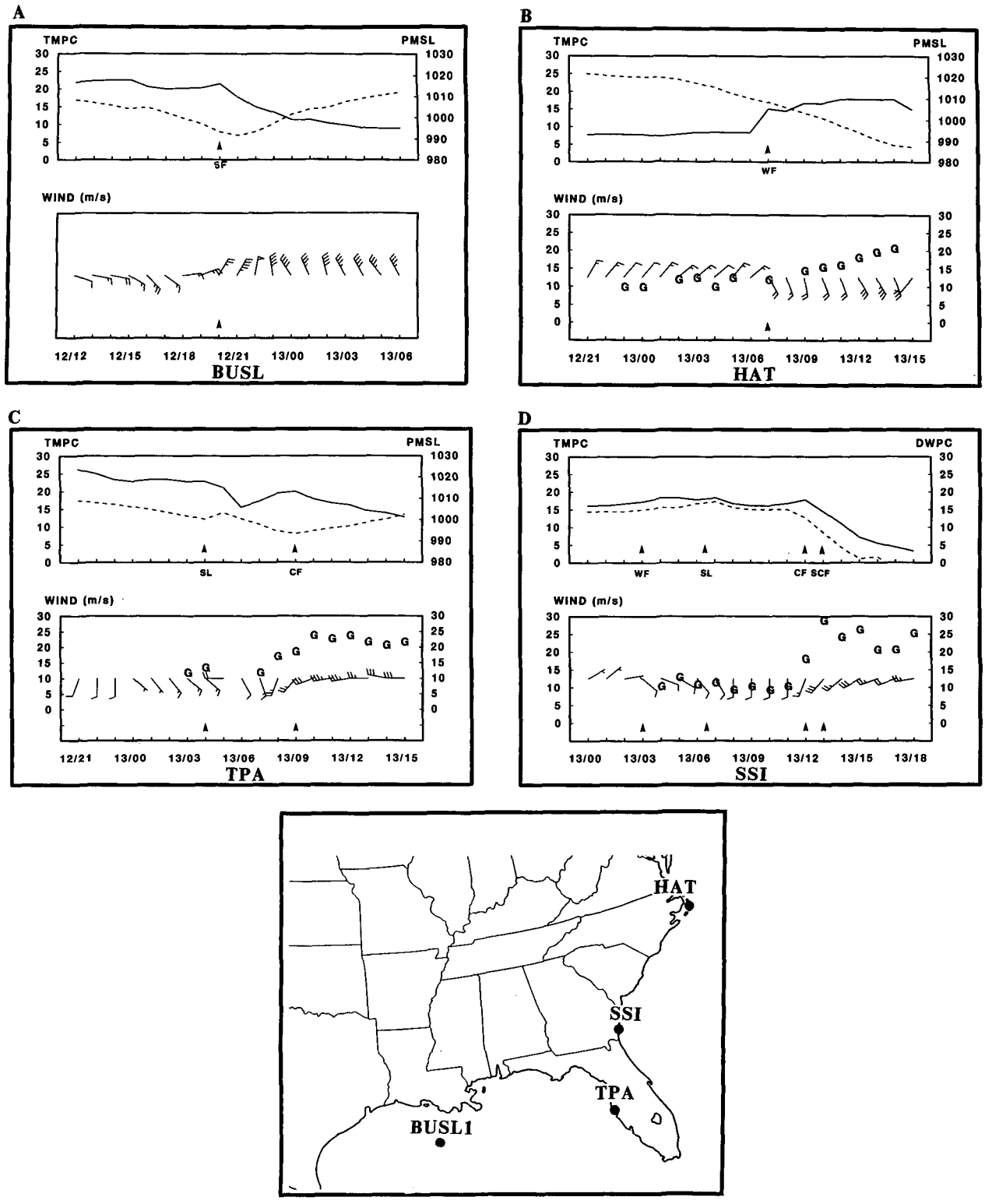

FIG. 11. (Top panel) Time series of temperature in °C (solid), pressure in mb (dashed); (bottom panel) wind speed, direction, and gust in m s^{-1}. Here SL—squall line passage, WF—warm frontal passage, CF—cold frontal passage, SCF—secondary cold frontal passage. (a) Bullwinkle oil platform (south of Louisiana coast), (b) Cape Hatteras, North Carolina, (c) Tampa, Florida, and (d) Brunswick/Mckinnon Airport, Georgia. [Note: top panel is temperature (solid), dewpoint (dashed).].

increase in wind speeds for coastal stations was not dramatic, approximately 5 m s^{-1}, but wind gusts increased significantly. Wind gusts at Cross City, Florida, approached 25 m s^{-1} after the frontal passage. There was little change in temperature (Fig. 11c) at this time. The coldest air remained behind a secondary cold front developing to the west of the storm center by 2100 UTC (Fig. 9b).

Although the primary cold front had propagated eastward, the strongest temperature gradients remained associated with the secondary cold front extending nearly parallel to the Texas and Louisiana coasts (Figs. 9b and 9c). The warming of the air behind the primary front moving toward Florida and ahead of the secondary front was perhaps the result of diabatic heating of the cold air that advected over the very warm waters of the Gulf of Mexico. The temperature gradient along the secondary front began to strengthen near the cyclone center by 0000 UTC 13 March and by 0900 UTC (Fig. 9f) was almost as strong as that analyzed along the warm front. This feature is similar to the bent-back warm front observed in other mature marine cyclones (Shapiro and Keyser 1990; Reed et al. 1992). As with other documented bent-back fronts, this feature is the location of the largest baroclinicity. In addition, the evolution of this feature is similar to that seen in other maritime cyclones. Observations and satellite imagery show the front beginning to wrap cyclonically around the storm, thus beginning the process of warm-air seclusion. A time series from Brunswick, Georgia (SSI), shows the signature that occurred with the frontal passages along the Atlantic coast (Fig. 11d). The primary front passed with a wind shift and decrease in dewpoint between 1100 and 1200 UTC but was no longer accompanied by a temperature change. As the secondary front moved through by 1300 UTC, there was a sharper decrease in temperature, and the wind gusts increased to 25 m s^{-1}.

3) Squall line

The development of the squall line that was accompanied by 11 tornadoes across Florida can be followed by examining the evolution of two surface troughs over the Gulf of Mexico on 12 March. The two troughs extended south from the cyclone center at 1200 UTC. A line of convection was associated with the western trough (T2) that slowly progressed eastward into the western Gulf of Mexico by 1800 UTC (Fig. 9a). The eastern (T1) trough had little or no convection associated with it, although it was marked by a wind shift from southeast to southwest and a secondary pressure minimum. The origin of both troughs is unknown and is beyond the scope of this paper.

During the afternoon, cumulus formed along T1, and by 2000 UTC a line of thunderstorms had developed. Observations of buoy 42001, located at 26°N, 90°W, showed a pressure fall of 4 mb in 2 h to 998.4 mb at 2000 UTC. As the gust front passed, the wind shifted to westerly, and at 2100 UTC this station was located in the downdraft near the mesoridge as the pressure rose 4 mb and the temperature dropped 7°C in 1 h. Thus, evidence exists for a presquall trough and a well-pronounced mesoridge collocated with the cold pool that often is associated with a squall line. However, there was no evidence for a wake low found in the observations. Rather, once the ridge passed, the pressure at the buoy continued to fall at the rate of 1–2 mb h^{-1} until the cold front reached the buoy. As the squall line moved past the buoy, the wind shifted back to a southerly direction and the temperature rose 5°C over the next 3 h.

The squall line approached the Florida coast between 0300 and 0600 UTC. There was evidence of increased inflow ahead of the thunderstorms as winds strengthened from the southeast, averaging 15 m s^{-1}. Both the mesotrough and mesoridge couplet propagated downstream with the squall line. The time series from Tampa, Florida (Fig. 11c), shows a secondary minimum and maximum in pressure as the squall line approached and passed the station. There was also a rapid drop in temperature and brief wind shift as the squall line passed. As occurred with buoy 42001, the wind returned to the synoptic-scale flow, while the temperature (and dewpoint) began to rise rapidly. In conjunction with the tornadic activity, the northern flank of the line bowed eastward across central and northern Florida. The squall line moved rapidly eastward and was located well off the Atlantic coast by 1200 UTC 13 March.

5. Summary

The superstorm of March 1993 was one of the most intense East Coast storms of the twentieth century. Few storms can match the cyclone's areal snowfall distribution, maximum snowfall, and number of low sea level pressure records observed during the storm. The storm developed as the result of an interaction between an upper-level short-wave trough and associated jet streak moving east toward the Gulf of Mexico and a second short-wave trough and polar jet that amplified as it propagated southeastward from the Rocky Mountain states to the Gulf Coast. The surface cyclone developed in the western Gulf of Mexico and intensified rapidly as it crossed the Gulf and moved ashore just west of Tallahassee, Florida. The movement and intensification of the cyclone as it propagated from the Gulf of Mexico to the East Coast was

accompanied by a tremendous amplification of the upper-level troughs over the eastern United States and Canada.

Precipitation spread rapidly northeastward from the Gulf Coast to much of the eastern seaboard as an upper-level jet streak amplified over the northeastern United States, its winds increasing from 60 to 90 m s^{-1} in only 12 h between 1200 UTC 12 March and 0000 UTC 13 March. Precipitation fell mainly as snow across the northern Gulf to the eastern Tennessee and Ohio Valleys and throughout much of the Middle Atlantic and New England states. The areal coverage of snowfall was among the largest of any storm in recorded history. Rain later changed to snow as far south as the Gulf Coast. As the storm headed for Florida, an intense squall line produced at least 11 tornadoes, and severe coastal flooding occurred as a surface cold front approached the west coast of Florida. A dramatic wind shift and increase in wind speed were observed with the passage of a cold front in western Florida, contributing to a 1.5–4-m storm surge observed along the northwestern Florida coast.

Mesoscale analyses focused on the development of the cyclone over the Gulf of Mexico. The cyclone deepened 29 mb in 24 h, not extraordinary for an Atlantic cyclone but equivalent to a 52-mb decrease at 60°N, when normalized for latitude according to Sanders and Gyakum (1980). The combination of an asymmetric pressure distribution, coupled with rapid deepening, resulted in exceptionally high winds north of the cyclone. In addition, cold-air damming east of the Appalachians and the warm Gulf Stream current provided precursor conditions for frontogenesis along the southeast coast, enhancing the low-level baroclinic zone along which the surface cyclone would continue to deepen as it moved northeastward.

As will be discussed in the companion papers (Caplan 1995; Uccellini et al. 1995), the observed deepening of this storm in the Gulf was not predicted well by any of the numerical models beyond 24 h prior to its development, although global models predicted a major East Coast storm 5 to 6 days in advance. The model deficiencies provide motivation for additional research on this storm. For example, documenting how the dynamic and diabatic processes acted to influence the precyclogenetic environment and enhance the rate of cyclogenesis over the Gulf of Mexico would make for an important study, both to understand better these processes and to provide insight into the model deficiencies for this case.

Acknowledgments. We would like to thank Scott Jacobs for his assistance in decoding data used throughout the paper. We would also like to thank Russell Schneider for his contributions to the research and critical reviews of the manuscript.

References

Bell, G. D., and L. F. Bosart, 1988: Appalachian cold-air damming. *Mon. Wea. Rev.*, **116,** 137–161.

Caplan, P., 1995: The 12–14 March 1993 superstorm: Performance of the global model. *Bull. Amer. Meteor. Soc.*, **76,** 201–212.

Chang, C. B., D. J. Perkey, and C. W. Kreitzberg, 1982: A numerical case study of the effects of latent heating on a developing wave cyclone. *J. Atmos. Sci.*, **39,** 1555–1570.

Davis, C. A., and K. A. Emanuel, 1991: Potential vorticity diagnostics of cyclogenesis. *Mon. Wea. Rev.*, **119,** 1929–1953.

Doyle, J. D., and T. J. Warner, 1993: A numerical simulation of coastal frontogenesis and mesoscale cyclogenesis during GALE IOP2. *Mon. Wea. Rev.*, **121,** 1048–1077.

Gyakum, J. R., 1983: On the evolution of the QEII storm. Part II: Dynamic and thermodynamic structure. *Mon. Wea. Rev.*, **111,** 1156–1173.

Keyser, D. A., and D. R. Johnson, 1984: Effects of diabatic heating on the ageostrophic circulation of an upper-tropospheric jet streak. *Mon. Wea. Rev.*, **112,** 1709–1724.

Kocin, P. J., 1983: An analysis of the blizzard of '88. *Bull. Amer. Meteor. Soc.*, 1258–1272.

——, and L. W. Uccellini, 1990: *Snowstorms along the Northeastern Coast of the United States: 1955 to 1985. Amer. Meteor. Soc.*, 280 pp.

——, A. D. Weiss, and J. J. Wagner, 1988: The great Arctic outbreak and East Coast blizzard of February 1899. *Wea. Forecasting*, **3,** 305–318.

Larsen, L. W., and E. L. Peck, 1974: Accuracy of precipitation measurements for hydrologic modeling. *Water Resour. Res.*, **4,** 857–863.

Lott, N., 1993: Water equivalent vs rain gauge measurements from the March 1993 blizzard. National Climatic Data Center Tech. Rep. 93–03.

Ludlum, D. L., 1968: *Early American Winters II: 1821–1870.* Amer. Meteor. Soc., 257 pp.

NWS, 1994: Superstorm of March 1993: March 12–14 1993. Natural disasters survey report, NWS, U.S. Dept. of Commerce, 152 pp.

Reed, R. J., J. Stoelinga, R. Mark, Y.-H. Kuo, 1992: A model-aided study of the origin and evolution of the anomalously high potential vorticity in the inner region of a rapidly deepening marine cyclone. *Mon. Wea. Rev.*, **120,** 893–913.

Sanders, F., and J. R. Gyakum, 1980: Synoptic–dynamic climatology of the "bomb." *Mon. Wea. Rev.*, **108,** 1589–1606.

Shapiro, M. A., and D. Keyser, 1990: Fronts, jet streams, and the tropopause. *Extratropical Cyclones: The Erik Palmén Memorial Volume,* C. Newton and E. Holopainen, Eds., Amer. Meteor. Soc., 166–191.

Uccellini, L. W., 1991: Processes contributing to the rapid development of extratropical cyclones. *Extratropical Cyclones: The Erik Palmén Memorial Volume,* C. Newton and E. Holopainen, Eds., Amer. Meteor. Soc., 81–107.

——, P. J. Kocin, R. S. Schneider, P. M. Stokols, and R. A. Dorr, 1995: Forecasting the 12–14 March 1993 superstorm. *Bull. Amer. Meteor. Soc.*, **76,** 183–199.

Whitaker, J. S., L. W. Uccellini, and K. F. Brill, 1988: A model-based diagnostic study of the rapid development phase of the Presidents' Day cyclone. *Mon. Wea. Rev.*, **116,** 431–451.